

SCIENTIFIC REPORTS



OPEN

Specific targeting of PKC δ suppresses osteoclast differentiation by accelerating proteolysis of membrane-bound macrophage colony-stimulating factor receptor

MiYeong Kim¹, Kyunghye Lee¹, Hong-In Shin² & Daewon Jeong¹

c-Fms is the macrophage colony-stimulating factor (M-CSF) receptor, and intracellular signalling via the M-CSF/*c-Fms* axis mediates both innate immunity and bone remodelling. M-CSF-induced transient proteolytic degradation of *c-Fms* modulates various biological functions, and protein kinase C (PKC) signalling is activated during this proteolytic process via an unknown mechanism. Notably, the role of specific PKC isoforms involved in *c-Fms* degradation during osteoclast differentiation is not known. Here, we observed that inactivation of PKC δ by the biochemical inhibitor rottlerin, a cell permeable peptide inhibitor, and short hairpin (sh) RNA suppresses osteoclast differentiation triggered by treatment with M-CSF and receptor activator of NF- κ B ligand. Interestingly, inhibition of PKC δ by either inhibitor or gene silencing of PKC δ accelerated M-CSF-induced proteolytic degradation of membrane-bound *c-Fms* via both the lysosomal pathway and regulated intramembrane proteolysis (RIPping), but did not affect *c-fms* expression at the mRNA level. Degradation of *c-Fms* induced by PKC δ inactivation subsequently inhibited M-CSF-induced osteoclastogenic signals, such as extracellular signal-regulated kinase (ERK), *c*-JUN N-terminal kinase (JNK), p38, and Akt. Furthermore, mice administered PKC δ inhibitors into the calvaria periosteum exhibited a decrease in both osteoclast formation on the calvarial bone surface and the calvarial bone marrow cavity, which reflects osteoclastic bone resorption activity. These data suggest that M-CSF-induced PKC δ activation maintains membrane-anchored *c-Fms* and allows the sequential cellular events of osteoclastogenic signalling, osteoclast formation, and osteoclastic bone resorption.

Macrophage colony-stimulating factor (M-CSF) mediates the differentiation of monocytic cells into phagocytic mononuclear macrophages relevant to osteoclast precursors, and subsequently participates in their survival, proliferation, and phagocytic function¹. The response to M-CSF is mediated by the M-CSF receptor tyrosine kinase, which is encoded by the *c-fms* proto-oncogene². Under normal physiological conditions, the binding of M-CSF to the extracellular domain of *c-Fms* elicits various signals that are required for the innate immune response, male and female fertility, osteoclast differentiation, and osteoclastic bone resorption^{3–5}. In contrast, excessive expression of M-CSF or *c-Fms* is associated with cancer development and metastasis as well as inflammatory diseases, such as atherosclerosis and rheumatoid arthritis^{6–8}. Mice lacking functional M-CSF or *c-Fms* show an osteopetrotic phenotype due to an osteoclast defect^{4,9}. In relation to bone metabolism, the data show that M-CSF and its cognate receptor *c-Fms* contribute to the proliferation and functional regulation of osteoclast precursor macrophages as well as osteoclast differentiation, and are thereby involved in bone remodelling.

¹Department of Microbiology, Laboratory of Bone Metabolism and Control, Yeungnam University College of Medicine, Daegu, 42415, Korea. ²IHBR, Department of Oral Pathology, School of Dentistry, Kyungpook National University, Daegu, 41940, Korea. Correspondence and requests for materials should be addressed to D.J. (email: dwjeong@ynu.ac.kr)

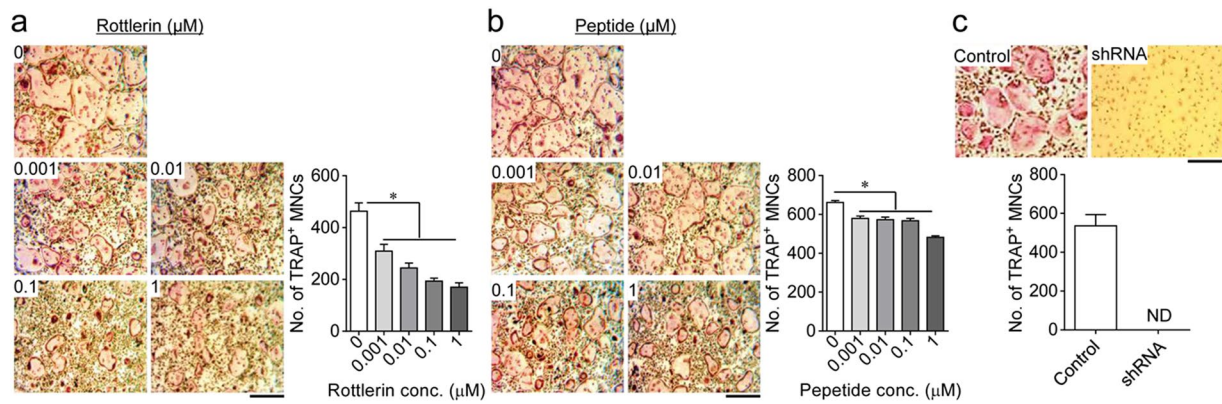


Figure 1. PKC δ inactivation inhibits osteoclast differentiation. **(a,b)** Osteoclast precursors were treated with a specific inhibitor of PKC δ (rottlerin or peptide inhibitor; ranging from 0 to 1 μ M) or dimethyl sulfoxide (control) and then differentiated into osteoclasts in the presence of M-CSF and RANKL for 4 days. **(c)** Osteoclast precursors were treated with a PKC δ -specific shRNA or a non-targeting shRNA (control) and then differentiated into osteoclasts by culturing with M-CSF and RANKL for 4 days. The extent of osteoclast differentiation was assessed by counting the number of TRAP-positive multinucleated osteoclasts (TRAP⁺ MNCs) with more than three nuclei. Data are mean \pm SD ($n = 3$). * $p < 0.01$ versus the control. ND, not detected. Scale bar, 500 μ m.

The biological function of the M-CSF/c-Fms axis is primarily regulated by the proteolytic degradation of plasma membrane-anchored c-Fms, which consists of five glycosylated extracellular immunoglobulin (Ig)-like domains, a single transmembrane region, and an intracellular tyrosine kinase domain¹⁰. When cellular signals induced by various stimulants are transmitted to c-Fms-harboring osteoclast precursor macrophages, c-Fms transiently disappears as a result of proteolytic degradation to restrict signal transduction and the subsequent cellular response¹¹. M-CSF, which directly interacts with c-Fms and affects various cellular functions, degrades c-Fms through two distinct lysosomal pathway and regulated intramembrane proteolysis (RIPping). In the lysosomal pathway, the M-CSF/c-Fms complex on the macrophage cell surface undergoes endocytosis and is degraded in the lysosome¹². Alternatively, c-Fms that becomes dimerised in response to M-CSF is rapidly degraded via RIPping¹³. This process is common for cell surface proteins, such as Fas and Fas ligand, IL-2 and IL-6 receptor, TNF α and receptor activator of NF- κ B ligand (RANKL)¹⁴. In addition, various pro-inflammatory agents, such as non-physiological compound 12-O-tetradecanoylphorbol-13-acetate (TPA; also known as phorbol 12-myristate 13-acetate or PMA)¹⁵ and pathogen products, such lipopolysaccharide (LPS), lipid A, lipoteichoic acid, and polyI:polyC, that can stimulate Toll-like receptors (TLRs)¹⁶ can induce RIPping of c-Fms. This is followed by serial cleavage of the extracellular and intracellular domains of c-Fms at the juxtamembrane region by TNF- α -converting enzyme (TACE) and γ -secretase, resulting in ectodomain shedding and release of the intracellular domain into the cytosol. RIPping of c-Fms induced by M-CSF, resulting in ectodomain shedding via TACE, limits the function of M-CSF by reducing receptor availability. After cleavage of the intracellular domain of c-Fms by γ -secretase, it is translocated to the nucleus, where it interacts with transcription factors that induce inflammatory gene expression¹⁷.

Several intracellular mediators that regulate c-Fms RIPping have been reported. Signalling by phospholipase C and protein kinase C (PKC) is required for the induction of c-Fms RIPping by macrophage activators (e.g., LPS, IL-2, and IL-4)¹⁸. In addition, the PKC activator TPA was shown to induce ectodomain shedding of c-Fms and other cell surface proteins, including TNF receptor, IL-6 receptor, CD14, CD16, CD43, and CD44^{18,19}. Among the various PKC isoforms, PKC β and PKC ϵ are involved in the respective regulation of heparin-binding EGF-like growth factor and TNF α shedding^{20,21} and PKC δ and PKC η are involved in regulating IL-6 receptor shedding²². These results indicate that PKC signalling may act as a positive regulator of ectodomain shedding during RIPping. In contrast to previous reports, we propose that M-CSF-mediated PKC δ activation negatively regulates lysosomal- and RIPping-dependent proteolytic degradation of the membrane-bound M-CSF receptor c-Fms, thereby retarding c-Fms proteolytic degradation, sustaining M-CSF-induced osteoclastogenic signalling, and stimulating osteoclast differentiation and osteoclastic bone resorption.

Results

PKC δ inactivation suppresses osteoclast differentiation. We previously reported that M-CSF is critical for osteoclast differentiation, and that it specifically activates PKC α and PKC δ ²³. To determine the role of PKC α and PKC δ signalling in osteoclast differentiation, osteoclast precursors were differentiated into multinucleated osteoclasts in the presence of M-CSF and RANKL for 4 days. Unfortunately, we failed to assess the functional involvement of PKC α in osteoclast differentiation, because the concentration of the specific PKC α inhibitor (Gö6976) that was required to inactivate PKC α had cytotoxic effects during osteoclast differentiation. Therefore, we focused on asking whether M-CSF-mediated PKC δ signalling modulated osteoclast differentiation. Treatment with the cell-permeable biochemical inhibitor rottlerin or the peptide inhibitor that targets PKC δ suppressed osteoclast formation (Fig. 1a,b), with no cytotoxic effects (Supplementary Fig. S1). This finding was

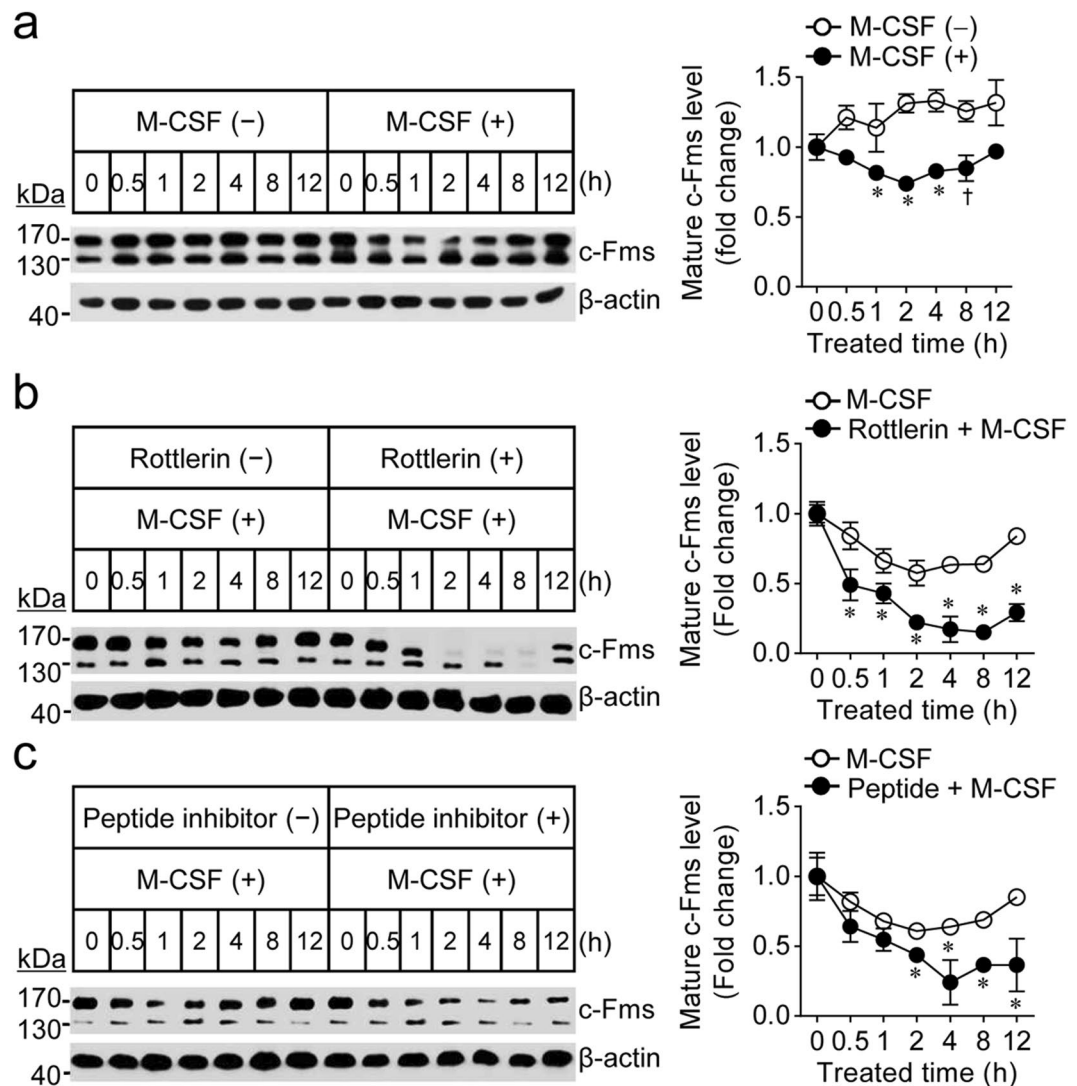


Figure 2. PKC δ inactivation accelerates M-CSF-induced proteolytic degradation of membrane-anchored c-Fms. (a–c) Osteoclast precursors were incubated in M-CSF-free medium for 4 h and treated with or without a specific inhibitor of PKC δ (rottlerin, 1 μ M or peptide inhibitor, 1 nM) for 30 min. Then, the cells were stimulated with or without M-CSF (30 ng/ml) for the indicated times. The levels of c-Fms were evaluated by immunoblot analysis. The fold changes in c-Fms (~170 kDa) were analysed by densitometry and normalised to β -Actin. Data are mean \pm SD (n = 3). * p < 0.01, † p < 0.05 versus the levels at 0 h.

also confirmed by PKC δ knockdown using a lentivirus carrying a short hairpin (sh) RNA (Fig. 1c). These results indicated that M-CSF-induced PKC δ activation mediates osteoclast differentiation.

Blocking of M-CSF-induced PKC δ activation downregulates the M-CSF receptor c-Fms. Consistent with previous reports², osteoclast precursors have two distinctive M-CSF receptor (c-Fms) types with different molecular weights, a 130 kDa precursor form that is present in the endoplasmic reticulum and a 170 kDa glycosylated mature form that is targeted to the plasma membrane. The mature c-Fms levels slightly decreased in response to M-CSF (Fig. 2a). In osteoclast precursors treated with both PKC δ inhibitor and M-CSF, the levels of mature c-Fms significantly decreased when compared with those treated with M-CSF alone, and then gradually increased to endogenous levels by 12 h after M-CSF exposure (Fig. 2b,c), supporting that PKC δ inactivation accelerates M-CSF-induced c-Fms proteolysis. This decrease was not observed in response to PKC δ inhibitor alone. In addition, we observed that shRNA-mediated PKC δ knockdown led to downregulation of c-Fms, depending on the levels of PKC δ (Fig. 3f). However, PKC δ inactivation did not affect c-Fms precursor protein levels. The combined results indicated that M-CSF-mediated PKC δ signalling maintains the level of mature, membrane-bound c-Fms.

Unexpectedly, we observed that inactivation of PKC δ by rottlerin also led to a progressive decrease in the molecular weight of mature c-Fms (Fig. 2b and Supplementary Fig. S2a,b), whereas inhibition of PKC δ by the peptide blocker or shRNA did not lead to a change in molecular weight. It is known that during maturation, c-Fms undergoes post-translational modifications, most likely N-linked glycosylation and phosphorylation². As

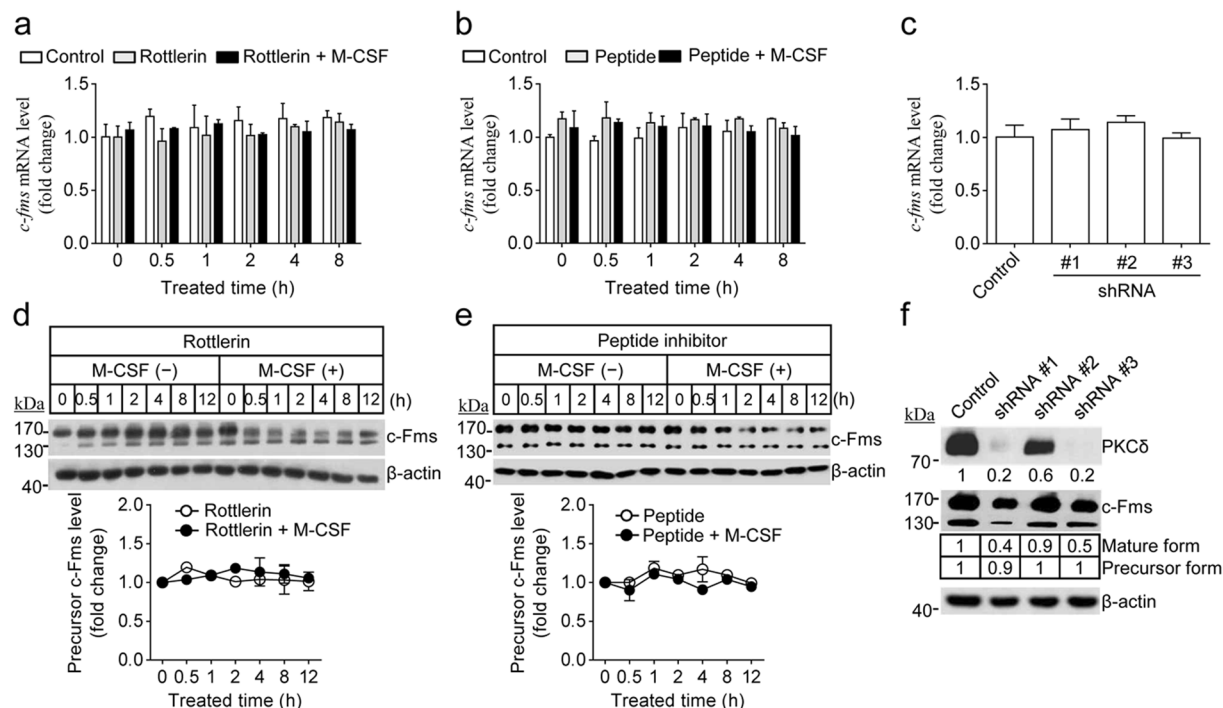


Figure 3. PKC δ inactivation did not affect the mRNA or de novo synthesised protein levels of c-Fms. (a–c) No change in *c-fms* mRNA levels following PKC δ inactivation. Osteoclast precursors were treated as described in Fig. 2. Then, relative *c-fms* mRNA levels were analysed by quantitative real-time PCR. Data are mean \pm SD ($n = 3$). (d,e) After cells were treated as described in Fig. 2a,b, levels of precursor *c-Fms* protein (~ 130 kDa) were determined by immunoblot analysis. (f) Osteoclast precursors treated with three independent PKC δ -specific shRNA clones were incubated with M-CSF for 12 h. Then, the efficiency of PKC δ knockdown and the levels of c-Fms were evaluated by immunoblot analysis. The fold changes in c-Fms (~ 130 and 170 kDa) and PKC δ were analysed by densitometry and normalised to β -Actin. Data are mean \pm SD ($n = 3$).

shown in Supplementary Fig. S2c,d, the reduction in the molecular mass of mature c-Fms induced by rottlerin seems to be dependent on the level of *N*-linked glycosylation, but not phosphorylation.

Next, we tested whether PKC δ inactivation regulates c-Fms at the transcriptional or translational levels. Inactivation of PKC δ by rottlerin, the peptide inhibitor, or shRNA at concentrations that downregulated mature c-Fms protein had no effect on *c-Fms* mRNA levels (Fig. 3a–c). Differing from the transient decrease observed in the mature c-Fms protein after exposure to PKC δ inhibitor or shRNA, c-Fms precursor protein levels did not change (Fig. 3d–f). These results indicated that the reduction in mature c-Fms induced by inhibition of PKC δ may be caused by degradation of membrane-anchored protein.

Proteolytic degradation of c-Fms induced by PKC δ inactivation leads to a defect in M-CSF-mediated osteoclastogenic signalling.

Degradation of c-Fms present in the plasma membrane is known occur via lysosomal proteolysis and/or TACE-mediated RIPPING^{12,13}. Therefore, we analysed the proteolytic process of c-Fms degradation caused by inhibition of PKC δ . The results showed that M-CSF-induced c-Fms degradation induced by inactivation of PKC δ was significantly blocked by treatment with chloroquine, an inhibitor of lysosomal degradation, or TAPI-0, a blocker of TACE-mediated RIPPING (Fig. 4a,b), indicating that PKC δ inhibition induces c-Fms degradation via both the lysosomal- and RIPPING-dependent pathways. Signalling via the M-CSF/c-Fms axis is known to be associated with osteoclast precursor proliferation and osteoclast survival. Thus, we assessed whether PKC δ inactivation controls M-CSF-mediated osteoclastogenic signalling during proteolytic degradation of c-Fms. As shown in Fig. 4c,d, the strength of the M-CSF-induced signals, including MAPKs and Akt, was markedly suppressed at a time point when c-Fms levels were maximally reduced by exposing both PKC δ inhibitor (rottlerin or peptide inhibitor) and M-CSF. This finding indicated that selective inactivation of PKC δ induced proteolytic degradation of c-Fms and led to a failure of osteoclastogenic signalling transmission via the M-CSF/c-Fms axis.

PKC δ inactivation inhibits osteoclast formation and bone resorption *in vivo*. Based on the suppressive effect of PKC δ inhibitor on osteoclast differentiation observed *in vitro*, we analysed whether PKC δ signalling affects osteoclast formation *in vivo*. Mice injected with a PKC δ inhibitor (rottlerin or peptide blocker) into the periosteal region of the calvaria daily for 5 days showed a decrease in the formation of tartrate-resistant acid phosphatase (TRAP)-positive mature osteoclasts on the bone surface within the calvarial bone marrow compared to control mice injected with PBS (Fig. 5a). Further histological analysis of calvarial sections stained with H&E revealed that mice administered the PKC δ inhibitor showed a reduction in the area of the calvarial bone marrow cavity, which reflects

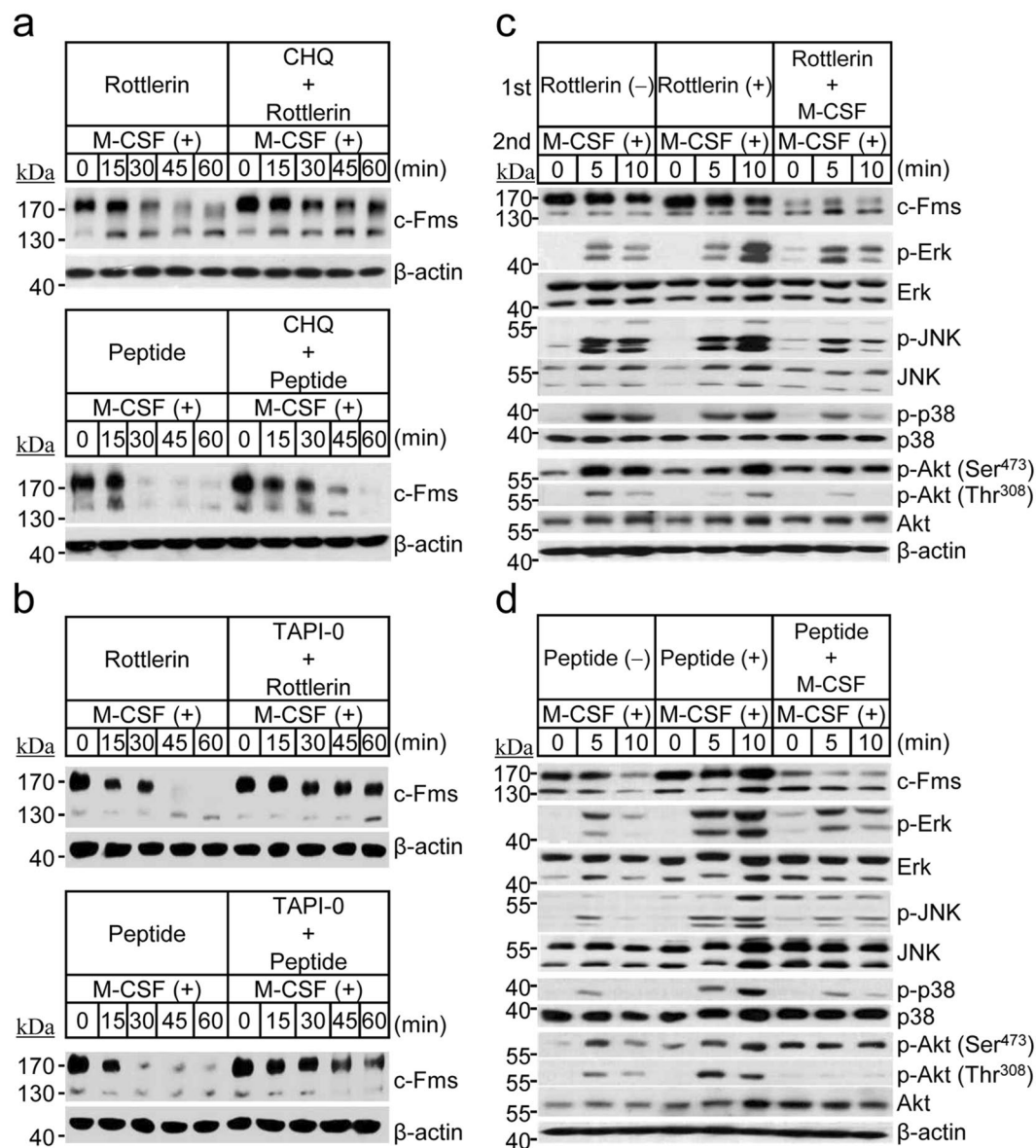


Figure 4. PKC δ inactivation potentiates the proteolytic degradation of c-Fms via both the lysosomal and RIPping pathways and suppresses M-CSF-induced osteoclastogenic signalling. **(a,b)** Osteoclast precursors were incubated in the absence of M-CSF for 4 h and then pretreated individually with the indicated inhibitors [PKC δ inhibitors, rottlerin (1 μ M) or peptide inhibitor (1 nM); lysosomal inhibitor, chloroquine (CHQ, 20 μ M); and an inhibitor of TACE-mediated RIPping, TAPI-0 (100 μ M)] for 30 min. Then, the cells were treated with or without M-CSF for the indicated times, and the levels of membrane-anchored c-Fms were determined by immunoblot analysis with an anti-c-Fms antibody. **(c,d)** Osteoclast precursors were exposed to M-CSF-depleted condition for 4 h. Firstly, cells were pre-incubated without or with a PKC δ inhibitor (rottlerin or peptide inhibitor) for 30 min and then treated in the presence or absence of M-CSF for 4 h to control the level of c-Fms. Secondly, cells were stimulated with M-CSF for 5 or 10 min and cell lysates were subjected to immunoblot analysis to determine the differential transmission of M-CSF-induced osteoclastogenic signalling. β -Actin was used as a loading control.

the bone-resorbing activity of osteoclasts, compared with this area in control mice (Fig. 5b). These results indicated that a PKC δ inhibitor can suppress osteoclast formation and bone resorption, and thus may be useful as a therapeutic agent for osteoporotic bone loss caused by the excessive bone resorbing activity of osteoclasts.

Discussion

In this study, we explored the role of PKC δ signalling in M-CSF-induced c-Fms proteolytic degradation during osteoclast differentiation. As shown in Fig. 5c, binding of M-CSF to its cognate receptor c-Fms activates PKC δ , which mediates osteoclast differentiation. M-CSF-mediated PKC δ activation maintains a steady level of membrane-bound c-Fms by preventing its proteolytic degradation via both the lysosomal pathway and RIPping.

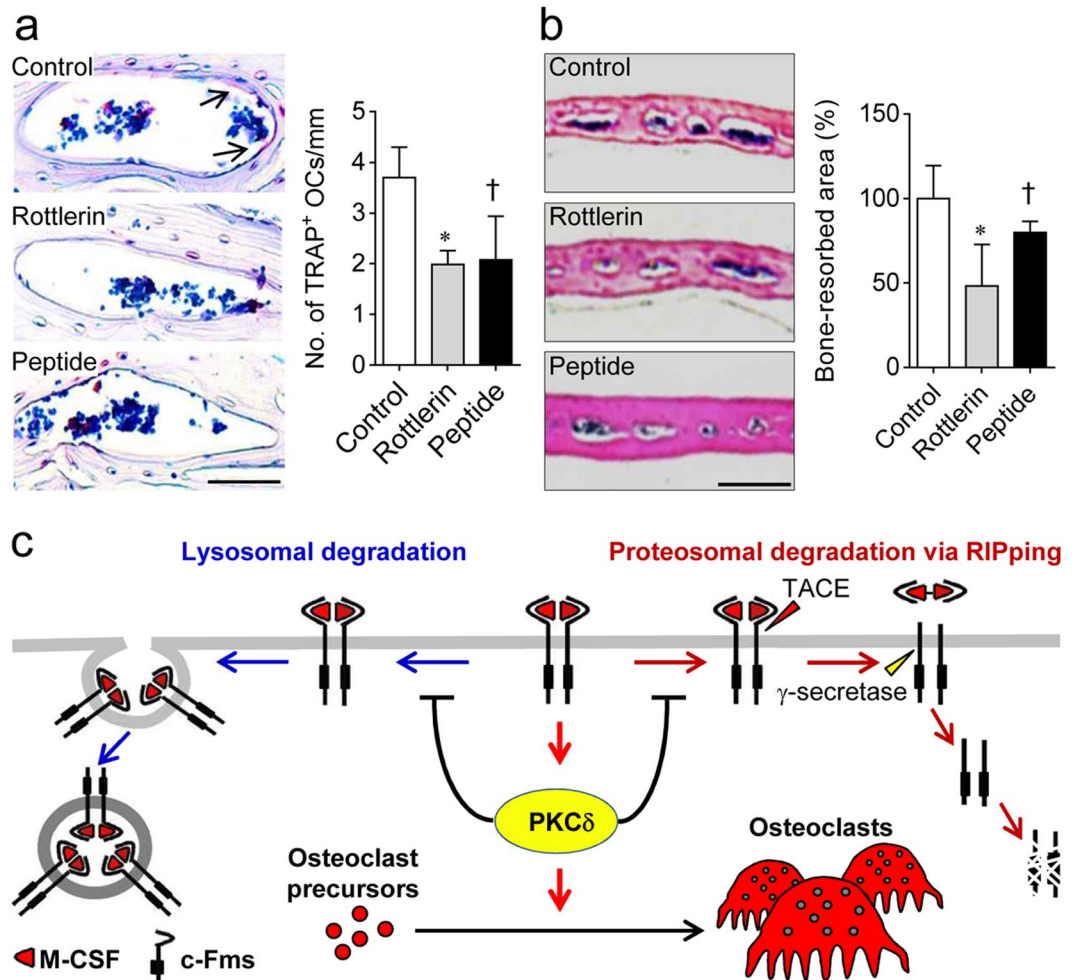


Figure 5. PKC δ inactivation suppresses osteoclast formation and osteoclastic bone resorption *in vivo*. Rottlerin (2 mg/kg), peptide inhibitor (5 mg/kg), or PBS (control) was injected into the calvarial periosteum of the mice daily for 5 days. Three days later, the mice were euthanised, and the calvaria were collected. **(a)** Osteoclast formation in calvaria. The calvarial sections were stained for TRAP, and the number of TRAP-positive osteoclasts on the calvarial bone surface was counted. Arrows indicate TRAP-positive osteoclasts. Scale bar, 50 μ m. **(b)** The bone marrow cavity in calvaria. H&E-stained sections were scanned, and the bone marrow cavity was measured. Scale bar, 1 mm. Data are mean \pm SD ($n = 5$). * $p < 0.01$, † $p < 0.05$ versus the control. **(c)** Schematic representation of the regulatory mechanism underlying the proteolytic degradation of membrane-anchored c-Fms via M-CSF-induced PKC δ activation.

This sequential process, via the M-CSF/c-Fms/PKC δ axis, sustains M-CSF-induced osteoclastogenic signalling, thereby inducing osteoclast formation and osteoclastic bone resorption under physiological conditions.

We previously showed that M-CSF stimulates PKC δ signalling²³. Here, we observed that membrane-bound c-Fms is degraded via M-CSF signalling under PKC δ inactivation; however, other forms of c-Fms protein were not degraded following inactivation of PKC δ . These combined results show that M-CSF-induced PKC δ activation controls c-Fms degradation to maintain appropriate levels of membrane-bound c-Fms by mediating intracellular signalling via the M-CSF/c-Fms axis. As shown in Supplementary Fig. S2d, treatment with M-CSF induced higher levels of tyrosine phosphorylation of several proteins, and this phenomenon was verified by adding the phosphatase inhibitor, Na₃VO₄, demonstrating that M-CSF led to an increase in kinase activity levels relative to phosphatase activity levels. In addition, PKC δ inhibitor treatment induced a decrease in tyrosine phosphorylation as well as decreased activation of MAPKs and Akt, other serine/threonine-specific protein kinase (Fig. 4c,d; Supplementary Fig. S2d). These findings indicated that M-CSF signalling controls various kinases, including MAPKs, Akt, and PKC δ , and that PKC δ activation participates in the regulation of these downstream kinases. Also, these results indicated that c-Fms regulation via M-CSF-induced PKC δ activation may be modulated by a dynamic interplay between kinases and phosphatases.

Studies have indicated that signalling via the M-CSF/c-Fms axis is tightly associated with the regulation of the immune system, cancer development^{24–26} and bone metabolism. In particular, osteopetrotic (op/op) mice lacking biologically active M-CSF and c-Fms-deficient mice exhibited retarded skeletal growth and osteopetrosis due to osteoclast malfunction^{4,9}. Many scientists have attempted to develop therapeutic drugs that target the

binding of M-CSF to c-Fms. However, such approaches had limitations, including the lack of a crystal structure for the M-CSF/c-Fms complex²⁷. Therefore, alternative therapeutic targets are needed. Here, we showed that selective targeting of PKC δ efficiently blocks osteoclastogenic signalling by accelerating c-Fms degradation, resulting in decreased osteoclast formation. Unexpectedly, we observed that inactivation of PKC δ by rottlerin led to lower molecular weight forms of membrane-bound c-Fms (Supplementary Fig. S2a). This seems to be caused by de-glycosylation of c-Fms, resulting from increased glycosidase activity (Supplementary Fig. S2c). In addition, our data and data from other studies have showed that rottlerin, at higher than nanomolar concentrations which are capable of inhibiting PKC δ , suppresses the activity of other protein kinases²⁸. The suppressive effect of rottlerin on protein kinase activity is poorly understood; therefore, it is not known whether PKC δ inactivation by rottlerin downregulates numerous downstream protein kinases or rottlerin acts non-specifically on other protein kinases in addition to PKC δ . For this reason, whether rottlerin is a specific inhibitor of PKC δ is still a matter of debate. However, we also showed that a specific cell-permeable peptide inhibitor of PKC δ did not affect the de-glycosylation of c-Fms, and the fact that a PKC δ -specific peptide inhibitor directly modulates other protein kinases has not been previously reported. Thus, this PKC δ inhibitory peptide may be better than rottlerin for the treatment of patients with osteoporotic bone defects caused by excessive osteoclast formation.

Our data showed that selective inhibition of PKC δ signalling accelerates the proteolytic degradation of the membrane-bound M-CSF receptor c-Fms, and thus suppresses osteoclast differentiation and bone resorption. Thus, exploring anti-osteoclastogenic agents capable of inducing c-Fms degradation will be useful for the development of alternative anti-osteoporotic drugs that can substitute for direct antagonists of c-Fms and inhibitors of the interaction between M-CSF and c-Fms.

Materials and Methods

Materials. A biochemical inhibitor (Rottlerin) and a peptide inhibitor [Δ PKC (8–17)] that specifically target PKC δ were purchased from Calbiochem (San Diego, CA, USA) and Anaspec, Inc. (Fremont, CA, USA), respectively. Primary antibodies were obtained from the following sources: c-Fms/CSF-1R (C-20), Akt, p-Akt^{Ser473}, p-Tyr (PY350), and β -actin from Santa Cruz Biotechnology (Dallas, TX, USA); PKC δ from BD Bioscience (San Jose, CA, USA); and Erk, p-Erk, JNK, p-JNK, p38, p-p38, and p-Akt^{Thr308} from Cell Signalling Technology (Danvers, MA, USA). All common reagents were from Sigma-Aldrich (St. Louis, MO, USA) unless otherwise specified.

Preparation of osteoclast precursors and osteoclast differentiation. Osteoclast precursors were isolated from the tibia and femur of 6-week-old C57BL/6 male mice (Koatech, Inc., Gyeonggido, Korea) by flushing the bone marrow as previously described²⁹. In brief, erythrocytes within the bone marrow fraction were lysed with red blood cell lysis buffer (Sigma-Aldrich). The remaining cells were cultured in alpha minimum essential medium (α -MEM; Hyclone, Logan, UT, USA) containing 10% foetal bovine serum (FBS, Hyclone), 1% antibiotic-antimycotic solution (Thermo Fisher Scientific, Inc., Waltham, MA, USA), and recombinant human M-CSF (5 ng/ml) for 12 h at 37°C in 5% CO₂. To generate osteoclast precursors, the floating cells were further cultured in α -MEM containing M-CSF (30 ng/ml) for 3 days. For osteoclast differentiation, osteoclast precursors (2.5×10^4 cells per well) were seeded onto 48-well culture plates and then differentiated into osteoclasts in the presence of M-CSF (30 ng/ml) and recombinant mouse RANKL (100 ng/ml) for 4 days. The medium was exchanged on day 2. To evaluate osteoclast differentiation, cells were stained for tartrate-resistant acid phosphatase (TRAP) using the Leukocyte Acid Phosphatase Staining Kit (Sigma-Aldrich) according to the manufacturer's instructions. TRAP-positive multinucleated cells (TRAP⁺ MNCs) with more than three nuclei were counted under a light microscope.

Knockdown of PKC δ by short hairpin RNA (shRNA). Lentiviral pLKO.1-puro expression plasmids encoding shRNA specific for PKC δ were purchased from Sigma-Aldrich (MISSION[®] shRNA plasmid DNA; clone IDs: NM_011103.1, NM_011103.2, and NM_011103.2). A pLKO.1-puro non-targeting shRNA plasmid was used as a control. Lentiviral particles were generated in HEK293T cells by co-transfection with compatible packaging plasmids encoding VSV-G and NL-BH, and shRNA-encoding plasmids using polyethylenimine (Polysciences, Inc., Warrington, PA, USA). After the culture medium containing lentivirus was passed through a 0.45 μ m syringe filter, osteoclast precursors were infected with lentivirus in the presence of polybrene (8 μ g/ml; Sigma-Aldrich) for 6 h, and then incubated in fresh medium containing M-CSF (60 ng/ml) and puromycin for selection (1 μ g/ml; Sigma-Aldrich) for 2 days. Puromycin-resistant cells were differentiated into osteoclasts in the presence of M-CSF (30 ng/ml) and RANKL (100 ng/ml) for 4 days.

Immunoblot analysis. Cells were lysed with a lysis buffer containing 50 mM Tris-HCl, pH 7.4, 150 mM NaCl, 1 mM EDTA, 1% Nonidet-P40, 1% SDS, 1 mM NaF, 1 mM Na₃VO₄, 1 mM β -glycerophosphate, and 1 \times protease inhibitor cocktail (Roche, Mannheim, Germany), and then the cell lysates were centrifuged at 10,000 \times g for 10 min at 4°C. The protein concentration of the resulting supernatants was determined using the DC protein assay (Bio-Rad, Hercules, CA, USA). Proteins (20 μ g) were separated by 10% SDS-PAGE, transferred to nitrocellulose membranes (GE Healthcare, Pittsburgh, PA, USA), and incubated with the primary antibodies as indicated. The antigen-antibody complexes were detected with appropriate horseradish peroxidase-conjugated secondary antibodies and ECL reagents (Abfrontier, Seoul, Korea). Fold changes were measured using Image J software 1.49 v (NIH, Bethesda, MD, USA).

Quantitative Real-time PCR. Total RNA was extracted from the cells using TRIzol reagent (Invitrogen, Carlsbad, CA, USA) and then reverse transcribed into cDNA using the M-MLV Reverse Transcription Kit (Invitrogen). Real-time polymerase chain reaction (PCR) was conducted in triplicate using Lightcycler[®] 480 SYBR Green I

Master Mix (Roche) and a Lightcycler 96 system (Roche). The levels of *c-fms* mRNA were analysed using the comparative delta threshold cycle method using glyceraldehyde-3-phosphate dehydrogenase (*GAPDH*) mRNA as an internal control. PCR primers were synthesised by Bionics Corp. (Seoul, Korea), and their sequences were as follows: mouse *c-fms* forward 5'-CAG AGC CCC CAC AGA TAA AA-3' and reverse 5'-GTC CAC AGC GTT GAG ACT GA-3'; mouse *GAPDH* forward 5'-AGG TCG GTG TGA ACG GAT TTG-3' and reverse 5'-TGT AGA CCA TGT AGT TGA GGT CA-3'.

Animal study. To assess the effects of the PKC δ inhibitors on calvarial bone remodelling, 8-week-old C57BL/6 male mice purchased from Koatech, Inc. were maintained in the mouse facility. All procedures using the mice were conducted in accordance with the Guide for the Care and Use of Laboratory Animals of Yeungnam University College of Medicine and were approved by the Institutional Animal Research Review Committee of Yeungnam University College of Medicine (permission number YUMC-AEC2016-038). Rottlerin (2 mg/kg), delta PKC (8–17) (5 mg/kg), or PBS (control) was injected onto the calvarial periosteum of the mice every day for 5 days, and then the mice were sacrificed on day 3 after the final injection. Calvarial specimens were surgically dissected from the mice, fixed in 3.7% formaldehyde, decalcified with EDTA solution, and sectioned using a microtome. The sections were then stained with TRAP to detect the osteoclasts on the calvarial bone surface and with haematoxylin and eosin (H&E) to visualise the bone marrow cavity, to assess osteoclastic bone-resorbing activity. The number of TPAP-positive osteoclasts was counted under a light microscope. To measure the area of the bone marrow cavity, which reflects osteoclastic bone-resorbing activity, images were scanned using an Aperio ScanScope (Model T3) and analysed using ImageScope software, version 6 (Aperio Technologies, Vista, CA, USA).

Statistical analysis. Quantitative data were expressed as the mean \pm SD of at least three independent experiments. Statistical analyses were performed using Student's two-tailed t-test for comparison between two groups or analysis of variance (ANOVA) and a post-hoc test for multiple comparisons using SPSS 21.0 software. *P* values less than 0.05 were considered statistically significant.

Data Availability

All data generated or analysed during this study are included in this published article (and its Supplementary Information files).

References

- Ushach, I. & Zlotnik, A. Biological role of granulocyte macrophage colony-stimulating factor (GM-CSF) and macrophage colony-stimulating factor (M-CSF) on cells of the myeloid lineage. *J Leukoc Biol* **100**, 481–489, <https://doi.org/10.1189/jlb.3RU0316-144R> (2016).
- Sherr, C. J. *et al.* The *c-fms* proto-oncogene product is related to the receptor for the mononuclear phagocyte growth factor, CSF-1. *Cell* **41**, 665–676 (1985).
- Stoy, N. Macrophage biology and pathobiology in the evolution of immune responses: a functional analysis. *Pathobiology* **69**, 179–211, <https://doi.org/10.1159/000055944> (2001).
- Dai, X. M. *et al.* Targeted disruption of the mouse colony-stimulating factor 1 receptor gene results in osteopetrosis, mononuclear phagocyte deficiency, increased primitive progenitor cell frequencies, and reproductive defects. *Blood* **99**, 111–120 (2002).
- Ryan, G. R. *et al.* Rescue of the colony-stimulating factor 1 (CSF-1)-nullizygous mouse (*Csf1*(op)/*Csf1*(op)) phenotype with a CSF-1 transgene and identification of sites of local CSF-1 synthesis. *Blood* **98**, 74–84 (2001).
- Ide, H. *et al.* Expression of colony-stimulating factor 1 receptor during prostate development and prostate cancer progression. *Proc Natl Acad Sci* **99**, 14404–14409, <https://doi.org/10.1073/pnas.222537099> (2002).
- Qiao, J. H. *et al.* Role of macrophage colony-stimulating factor in atherosclerosis: studies of osteopetrotic mice. *Am J Pathol* **150**, 1687–1699 (1997).
- Paniagua, R. T. *et al.* *c-Fms*-mediated differentiation and priming of monocyte lineage cells play a central role in autoimmune arthritis. *Arthritis Res* **12**, R32, <https://doi.org/10.1186/ar2940> (2010).
- Yoshida, H. *et al.* The murine mutation osteopetrosis is in the coding region of the macrophage colony stimulating factor gene. *Nature* **345**, 442, <https://doi.org/10.1038/345442a0> (1990).
- Li, W. & Stanley, E. R. Role of dimerization and modification of the CSF-1 receptor in its activation and internalization during the CSF-1 response. *EMBO J* **10**, 277–288 (1991).
- Lee, K. *et al.* Blocking of the Ubiquitin-Proteasome System Prevents Inflammation-Induced Bone Loss by Accelerating M-CSF Receptor *c-Fms* Degradation in Osteoclast Differentiation. *Int J Mol Sci* **18**, <https://doi.org/10.3390/ijms18102054> (2017).
- Lee, P. S. *et al.* The *Cbl* protooncogene stimulates CSF-1 receptor multiubiquitination and endocytosis, and attenuates macrophage proliferation. *EMBO J* **18**, 3616–3628, <https://doi.org/10.1093/emboj/18.13.3616> (1999).
- Glenn, G. & van der Geer, P. CSF-1 and TPA stimulate independent pathways leading to lysosomal degradation or regulated intramembrane proteolysis of the CSF-1 receptor. *FEBS Lett* **581**, 5377–5381, <https://doi.org/10.1016/j.febslet.2007.10.031> (2007).
- Hayashida, K., Bartlett, A. H., Chen, Y. & Park, P. W. Molecular and cellular mechanisms of ectodomain shedding. *Anat Rec (Hoboken)* **293**, 925–937, <https://doi.org/10.1002/ar.20757> (2010).
- Wilhelmsen, K. & van der Geer, P. Phorbol 12-myristate 13-acetate-induced release of the colony-stimulating factor 1 receptor cytoplasmic domain into the cytosol involves two separate cleavage events. *Mol Cell Biol* **24**, 454–464 (2004).
- Glenn, G. & van der Geer, P. Toll-like receptors stimulate regulated intramembrane proteolysis of the CSF-1 receptor through Erk activation. *FEBS Lett* **582**, 911–915, <https://doi.org/10.1016/j.febslet.2008.02.029> (2008).
- Fortini, M. E. Gamma-secretase-mediated proteolysis in cell-surface-receptor signalling. *Nat Rev Mol Cell Biol* **3**, 673–684, <https://doi.org/10.1038/nrm910> (2002).
- Rovida, E., Paccagnini, A., Del Rosso, M., Peschon, J. & Dello Sbarba, P. TNF-alpha-converting enzyme cleaves the macrophage colony-stimulating factor receptor in macrophages undergoing activation. *J Immunol* **166**, 1583–1589 (2001).
- Hooper, N. M., Karran, E. H. & Turner, A. J. Membrane protein secretases. *Biochem J* **321**(Pt 2), 265–279 (1997).
- Izumi, Y. *et al.* A metalloprotease-disintegrin, MDC9/meltrin-gamma/ADAM9 and PKCdelta are involved in TPA-induced ectodomain shedding of membrane-anchored heparin-binding EGF-like growth factor. *EMBO J* **17**, 7260–7272, <https://doi.org/10.1093/emboj/17.24.7260> (1998).
- Wheeler, D. L., Ness, K. J., Oberley, T. D. & Verma, A. K. Protein kinase Cepsilon is linked to 12-O-tetradecanoylphorbol-13-acetate-induced tumor necrosis factor-alpha ectodomain shedding and the development of metastatic squamous cell carcinoma in protein kinase Cepsilon transgenic mice. *Cancer Res* **63**, 6547–6555 (2003).

22. Thabard, W., Collette, M., Bataille, R. & Amiot, M. Protein kinase C delta and eta isoenzymes control the shedding of the interleukin 6 receptor alpha in myeloma cells. *Biochem J* **358**, 193–200 (2001).
23. Kim, J. M., Kim, M. Y., Lee, K. & Jeong, D. Distinctive and selective route of PI3K/PKCalpha-PKCdelta/RhoA-Rac1 signaling in osteoclastic cell migration. *Mol Cell Endocrinol* **437**, 261–267, <https://doi.org/10.1016/j.mce.2016.08.042> (2016).
24. Lin, E. Y., Gouon-Evans, V., Nguyen, A. V. & Pollard, J. W. The macrophage growth factor CSF-1 in mammary gland development and tumor progression. *J Mammary Gland Biol Neoplasia* **7**, 147–162 (2002).
25. Escamilla, J. *et al.* CSF1 receptor targeting in prostate cancer reverses macrophage-mediated resistance to androgen blockade therapy. *Cancer Res* **75**, 950–962, <https://doi.org/10.1158/0008-5472.CAN-14-0992> (2015).
26. Sluiter, M. *et al.* Inhibition of CSF-1R supports T-cell mediated melanoma therapy. *PLoS One* **9**, e104230, <https://doi.org/10.1371/journal.pone.0104230> (2014).
27. Rosenfeld, L. *et al.* Combinatorial and Computational Approaches to Identify Interactions of Macrophage Colony-stimulating Factor (M-CSF) and Its Receptor c-FMS. *J Biol Chem* **290**, 26180–26193, <https://doi.org/10.1074/jbc.M115.671271> (2015).
28. Soltoff, S. P. Rottlerin: an inappropriate and ineffective inhibitor of PKCdelta. *Trends Pharmacol Sci* **28**, 453–458, <https://doi.org/10.1016/j.tips.2007.07.003> (2007).
29. Huh, Y. J. *et al.* Regulation of osteoclast differentiation by the redox-dependent modulation of nuclear import of transcription factors. *Cell Death Differ* **13**, 1138–1146, <https://doi.org/10.1038/sj.cdd.4401793> (2006).

Acknowledgements

This work was supported by grants from the Korea Healthcare Technology R&D Project, Ministry for Health, Welfare, Family Affairs, Republic of Korea (No. HI15C2164), and the National Research Foundation of Korea (Nos 2016R1A2B2012108 and 2015R1A5A2009124).

Author Contributions

D.J. designed experiments, analyzed the data and wrote the manuscript. M.Y.K. and K.L. performed the experiments and analyzed data. H.I.S. helped to data analysis.

Additional Information

Supplementary information accompanies this paper at <https://doi.org/10.1038/s41598-019-43501-2>.

Competing Interests: The authors declare no competing interests.

Publisher's note: Springer Nature remains neutral with regard to jurisdictional claims in published maps and institutional affiliations.



Open Access This article is licensed under a Creative Commons Attribution 4.0 International License, which permits use, sharing, adaptation, distribution and reproduction in any medium or format, as long as you give appropriate credit to the original author(s) and the source, provide a link to the Creative Commons license, and indicate if changes were made. The images or other third party material in this article are included in the article's Creative Commons license, unless indicated otherwise in a credit line to the material. If material is not included in the article's Creative Commons license and your intended use is not permitted by statutory regulation or exceeds the permitted use, you will need to obtain permission directly from the copyright holder. To view a copy of this license, visit <http://creativecommons.org/licenses/by/4.0/>.

© The Author(s) 2019